# Orbital Glass State of the Nearly Metallic Spinel Cobalt Vanadate

R. Koborinai, S. E. Dissanayake, M. Reehuis, M. Matsuda, T. Kajita, H. Kuwahara, S.-H. Lee, and T. Katsufuji

Phys. Rev. Lett. **116**, 037201 — Published 19 January 2016

DOI: 10.1103/PhysRevLett.116.037201

# Orbital glass state of the nearly metallic spinel cobalt vanadate

R. Koborinai,[1] S.E. Dissanayake,[2,*] M. Reehuis,[3] M. Matsuda,[4]
T. Kajita,[1] H. Kuwahara,[5] S. -H. Lee,[2] and T. Katsufuji[1,6,†]

[1]*Department of Physics, Waseda University, Tokyo 169-8555, Japan*
[2]*Department of Physics, University of Virginia, Charlottesville, Virginia 22904, USA*
[3]*Helmholtz-Zentrum für Materialien und Energie, 14109 Berlin, Germany*
[4]*Quantum Condensed Matter Division, Oak Ridge National Laboratory, Oak Ridge, TN 37831, USA*
[5]*Department of Physics, Sophia University, Tokyo 102-8554, Japan*
[6]*Kagami Memorial Research Institute for Materials Science and Technology, Waseda University, Tokyo 169-0051, Japan*

(Dated: December 23, 2015)

Strain, magnetization, dielectric relaxation, and unpolarized and polarized neutron diffraction measurements were performed to study the magnetic and structural properties of spinel $Co_{1-x}V_{2+x}O_4$. The strain measurement indicates that upon cooling, $\Delta L/L$ in the order of $\sim 10^{-4}$ starts increasing below $T_C$, becomes maximum at $T_{max}$, and then decreases and changes its sign at $T^*$. Neutron measurements indicate that a collinear ferri-magnetic order develops below $T_C$ and upon further cooling non-collinear ferri-magnetic ordering occurs below $T_{max}$. At low temperatures, the dielectric constant exhibits a frequency dependence, indicating a slow dynamics. These results indicate the existence of an orbital glassy state at low temperatures in this nearly metallic frustrated magnet.

PACS numbers: 75.25.Dk,75.25.-j,75.80.+q,75.50.Gg

The interplay between magnetic frustration and orbital degree of freedom has been extensively studied in various transition-metal oxides. Among them, spinel vanadates $AV_2O_4$, in which the magnetic $V^{3+}$ ($t_{2g}^2$) ions form a highly frustrated three-dimensional corner-sharing network of tetrahedra, are model systems to search for novel emergent phases. With non-magnetic $A^{2+}$ ions ($A$ = Zn, Cd), upon cooling the system undergoes a first order structural phase transition due to an orbital long range order followed by a bi-partite magnetic order[1–3]. With magnetic $A^{2+}$ ions such as Mn, Fe and Co, additional spin exchange interactions between $A^{2+}$ and $V^{3+}$ ions come into play to exhibit more complex behaviors. For example, the insulating $MnV_2O_4$ [4–13] exhibits a first order structural phase transition from cubic to tetragonal (with a shorter $c$ axis) and ferrimagnetic order with a noncollinear V spin structure [7] simultaneously at $T_C = 57$ K. This phase transition is dominated by the Kugel-Khomskii-type interactions that are the intersite interactions between orbital and spin degrees of freedom of the V ions. Another insulating $FeV_2O_4$ [14–22] exhibits, upon cooling, successive structural phase transitions from a cubic to a high-temperature tetragonal to an orthorhombic, and to a low-temperature tetragonal phase (with a longer $c$ axis), which are caused not only by the orbital degree of freedom of V ions but also of $Fe^{2+}$ ($3d^6$; $e_g^3 t_{2g}^3$) ions [14]. In both compounds, the orbital ordering of the V ions seems to be accompanied by the canting of the V spins [7, 16].

Spinel cobalt vanadate $Co_{1+x}V_{2-x}O_4$ ($Co^{2+}$: $e_g^4 t_{2g}^3$, $V^{3+}$: $t_{2g}^2$) provides a unique situation due to its close proximity to itineracy [23–29]. Unlike in the insulating $AV_2O_4$ ($A$ = Mn, Fe), no crystal distortion has been observed in the spinel cobalt vanadate down to 10 K by x-ray diffraction, while a similar ferrimagnetic order as in the insulating compounds was detected below $T_C \simeq 150$ K by the dc bulk magnetization ($M_{bulk}$) [23]. More recently, a neutron scattering study on $Mn_{1-y}Co_yV_2O_4$ proposed, by extrapolating from $y \leq 0.8$, the disappearance of orbital order for higher Co concentration ($y \geq 0.8$) due to the enhancement of itineracy [28]. On the other hand, the $M_{bulk}(T)$ data obtained from polycrystalline samples of $CoV_2O_4$ showed two cusps centered at 60 and 100 K, and the specific heat $C_p(T)$ exhibited one peak at 60 K and a broad peak centered at $T_C$, which was attributed to a short-range orbital order [25]. This contradicts a previous single crystal study of $Co_{1+x}V_{2-x}O_4$ that reported one cusp in $M_{bulk}(T)$ at 75 K and no corresponding anomaly in $C_p(T)$ [24], which was attributed to the orbital glass order [25]. The seemingly conflicting results might be due to the offstoichiometry of the samples, which has complicated the understanding of the system. Nonetheless, the anomalies below $T_C$ observed in the different measurements suggest that the orbital degree of freedom might be playing an important role also in this compound although the associated lattice distortion might be too small to be easily detected. This calls for the use of experimental probes that are more sensitive to such subtle changes in magnetic and structural properties that might exist in this nearly metallic spinel.

In this paper, we report the strain, magnetization, dielectric relaxation, and unpolarized and polarized neutron diffraction measurements of spinel cobalt vanadate $Co_{1+x}V_{2-x}O_4$ in the single crystalline forms ($x = 0.16$, 0.21, and 0.30) and in the polycrystalline forms ($0 \leq x \leq 0.3$) to investigate the intrinsic properties of the system that are irrespective of the offstoichiometry. Our strain

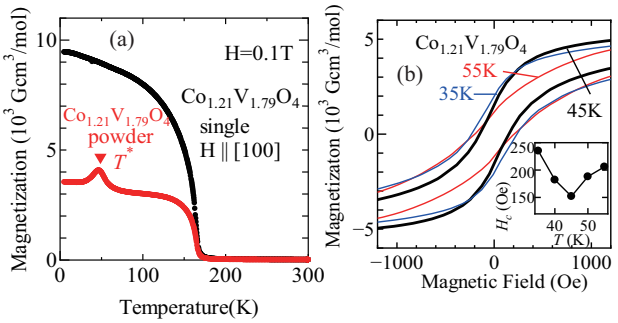


FIG. 1: (Color online) (a) $T$ dependence of magnetization, $M_{\rm bulk}(T)$ for a single crystal of $Co_{1.21}V_{1.79}O_4$ (#1) with an applied field $H$ of 0.1 T along the [100] axis and that for powder sample obtained by grinding the single crystal. (b) $M_{\rm bulk}$ vs $H$ for a ground single crystal of $Co_{1.21}V_{1.79}O_4$ around $T^* = 45$ K. The inset shows the $T$ dependence of coercive field, $H_c$.

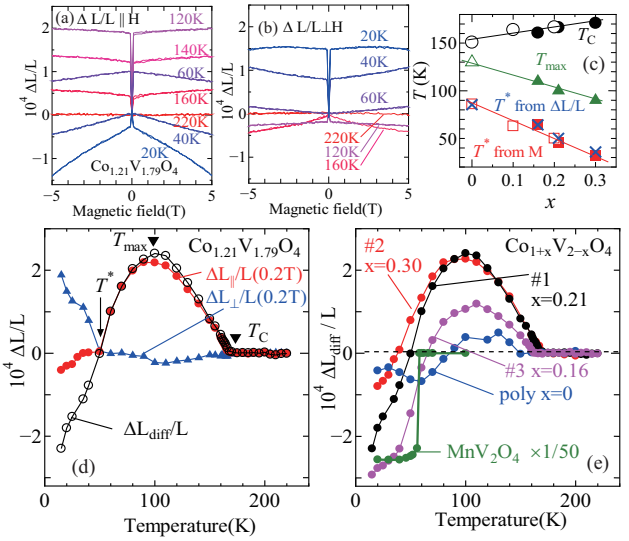


FIG. 2: (Color online) $H$-dependence of strain ($\Delta L/L$) for $Co_{1.21}V_{1.79}O_4$ (#1) at various $T$ (a) parallel to $H$, $\Delta L_\parallel/L$, and (b) perpendicular to $H$, $\Delta L_\perp/L$. (c) The $x$ dependence of $T_{\rm C}$ (circles), $T^*$ (squares from $M(T)$ and crosses from $\Delta L/L$), and $T_{\rm max}$ (triangles) for single crystals (solid symbols) and polycrystalline samples (open symbols) of $Co_{1+x}V_{2-x}O_4$. (d) $T$ dependence of $\Delta L/L \parallel H$ (closed circles), $\Delta L/L \perp H$ (triangles), and the difference of the two, $\Delta L_{\rm diff}/L$ (open circles). (e) Difference in the strain, $\Delta L_{\rm diff}/L = (\Delta L_\parallel - \Delta L_\perp)/L$ as a function of $T$ for various $Co_{1+x}V_{2-x}O_4$ samples. For comparison, $c/a - 1$ obtained by the x-ray diffraction measurement for $MnV_2O_4$ (multiplied by 1/50) is also shown.

data $\Delta L/L$ shows that upon cooling, a subtle distortion of the crystal $\Delta L/L \sim 10^{-4}$ is maximized at $T_{\rm max}$, and changes its sign at $T^*$ from positive to negative, i.e., the distortion changes from elongation to contraction in a second-order fashion. The canting of the V spins starts to evolve, far below $T_{\rm C}$, $\sim T_{\rm max}$ . Such a small distortion of the crystal associated with the change in the spin structure, together with the frequency dependence of the dielectric constant observed at low $T$s, indicate that an orbital glassy order occurs at low $T$s in this nearly metallic frustrated magnet.

Details of the experimental preparations and setups are described in the Supplementary Material[29].

Fig. 1 (a) shows the temperature ($T$) dependence of $M_{\rm bulk}$ obtained from a single crystal of $Co_{1.21}V_{1.79}O_4$ (#1) with an applied magnetic field ($H$) of 0.1 T along the [100] direction. $M_{\rm bulk}(T)$ increases below the ferrimagnetic transition temperature $T_{\rm C} \sim 165$ K (black circles). Unlike in the case of polycrystalline samples, anomalies in $M_{\rm bulk}(T)$ below $T_{\rm C}$ are barely visible in the single crystal data. When the same crystal was ground to a powder, however, $M_{\rm bulk}(T)$ exhibits a clear anomaly at $T^* = 45$ K (red circles). Similar peaks are observed in $Co_{1+x}V_{2-x}O_4$ with various values of $x$ as shown in the supplementary material [29]. Fig. 1 (b) shows that $M_{\rm bulk}(H)$ exhibits a hysteresis due to the presence of ferromagnetic components, and that the $T$-dependence of the coercive field $H_c$ at which $M$ becomes zero. $H_c(T)$ exhibits a dip centered at $T^* = 45$ K for $x = 0.21$.

Figures 2 (a)(b)(d) show the strain ($\Delta L/L$) data obtained from the #1 $x = 0.21$ single crystal when the magnetic field, $H \parallel [100]$, is applied, as a function of $H$ and $T$. Upon ramping up, the strain, both parallel ($\Delta L_\parallel/L$) and perpendicular ($\Delta L_\perp/L$) to $H$, do not show any response to $H$ for $T = 220\,{\rm K} > T_{\rm C}$. Below $T_{\rm C}$, however, the strain exhibits a strong response. Interestingly, the strain response to $H$ shows an opposite behavior between the two $T$ regimes, above and below $T^*$. For $T^* \lesssim T < T_{\rm C}$, as $|H|$ increases up to 0.2 T, $\Delta L_\parallel/L$ sharply increases (Fig. 2 (a)) while $\Delta L_\perp/L$ sharply decreases by a much smaller amount (Fig. 2 (b)). Upon further ramping, the change in $\Delta L/L$ becomes gradual. For $T \lesssim T^*$, however, the strain response is opposite; upon ramping up to 0.2 T, $\Delta L_\parallel/L$ sharply decreases by a small amount while $\Delta L_\perp/L$ sharply increases by a much larger amount.

The $T$-dependence of the sharp response at the low field of $|H| = 0.2$ T is shown in Fig. 2 (d). Upon cooling, $\Delta L_\parallel/L$ $(T, |H| = 0.2$ T) (red circles) starts increasing gradually below $T_{\rm C}$, and reaches its maximum value of $\sim 2 \times 10^{-4}$ at $\sim 100$ K. Upon further cooling, it decreases and becomes negative below 45 K. $\Delta L_\perp/L(T, |H| = 0.2$ T) (blue triangles), on the other hand, behaves almost opposite to $\Delta L_\parallel/L$. Their difference, $\Delta L_{\rm diff}/L = (\Delta L_\parallel - \Delta L_\perp)/L$ (open circles) is a measure of distortion from the cubic phase, $\frac{c}{a} - 1$, assuming that the total magnetic moments of the Co and V ions are along the $c$ direction of the tetragonal crystal. There are two characteristic temperatures in $\Delta L_{\rm diff}/L$ of $Co_{1+x}V_{2-x}O_4$ below $T_{\rm C}$; $T_{\rm max}$ at which $\Delta L_{\rm diff}/L$ is maximized, and $T^*$ at which $\Delta L_{\rm diff}/L$ crosses zero (Fig. 2 (d) and (e)) and $M_{\rm bulk}(T)$ exhibit a peak (Fig. 1 (a)).

$\Delta L_{\rm diff}/L$ with other values of $x$ in $Co_{1+x}V_{2-x}O_4$ are shown in Fig. 2 (e), and the $x$ dependence of $T_{\rm C}$, $T_{\rm max}$,

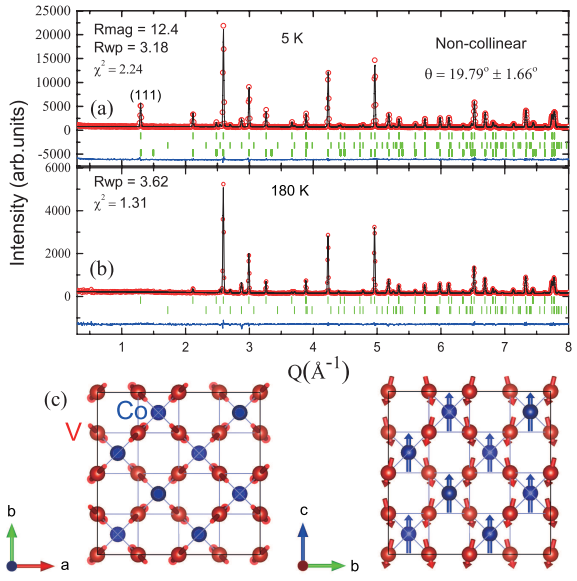


FIG. 3: (Color online) Neutron diffraction on a stoichiometric $CoV_2O_4$ powder sample, measured at (a) 5 K and (b) 180 K. Circles are the experimental data and black lines represent the calculated intensities. Green bars represent nuclear and magnetic Bragg peak positions and blue lines represent the difference between the experiment and the calculation. (c) A sketch of the ferrimagnetic structure refined with the 5 K data.

and $T^*$ is shown in Fig. 2 (c). Note that the coincidence between $T^*$ estimated from $\Delta L_{\rm diff}/L$ and that from $M(T)$ is commonly observed in $Co_{1+x}V_{2-x}O_4$ with other $x$ values. Both $T^*$ and $T_{\rm max}$ increases with decreasing $x$, and $T^*$ for $x = 0$ (85 K) is close to $T$ where an anomaly of the lattice constant was observed in a recent neutron diffraction study on a polycrystalline sample of $CoV_2O_4$[30]. It should also be pointed out that the gradual change in $\Delta L_{\rm diff}/L$ in $Co_{1+x}V_{2-x}O_4$ starkly contrasts with the sharp first-order contraction due to the long range orbital ordering at 57 K observed in $MnV_2O_4$ [green circles in Fig. 2 (e)], suggesting a glassy nature of the orbital ordering in $Co_{1+x}V_{2-x}O_4$.

To investigate how the magnetic state evolves with the changes in the crystal structure, neutron diffraction experiments were performed on polycrystalline and single crystal samples. Figure 3 (a) shows the neutron powder diffraction data collected at 5 K ($< T_{\rm C}$) and 180 K ($> T_{\rm C}$) for stoichiometric polycrystalline $CoV_2O_4$. The overall crystal structure remains cubic with $Fd\bar{3}m$ symmetry down to 5 K. An obvious difference between the 5 K and 180 K data is the strong (111) Bragg intensity at 5 K, which is due to the ferrimagnetic order with the characteristic wave vector of $\mathbf{k}_m = (0, 0, 0)$. The refinement of the diffraction data at 5 K indicates that the $Co^{2+}$ magnetic moments are ferromagnetically aligned along one principal axis of the cubic spinel, defined as the $c$-axis, and the $c$-component of the $V^{3+}$ moments are antiparallel to the $Co^{2+}$ moments. In addition, the V moments are canted from the $c$-axis by $\sim 20(2)^\circ$ to the $\langle 110 \rangle$ direction, and the $ab$-plane components of the neighboring $V^{3+}$ moments are antiferromagnetically aligned with each other. This magnetic structure is reproducible by the $\Gamma_9$ irreducible representation for the $Fd\bar{3}m$ space group with $\mathbf{k}_m = (0, 0, 0)$, as illustrated in Figs. 3 (c). This magnetic structure is similar to that of $FeV_2O_4$ at low $T$s [16]. The magnitude of the ordered Co moment at 5 K, $\langle M_{\rm Co} \rangle = 2.89(3)\mu_{\rm B}$, is close to the expected value for the high-spin state of $Co^{2+}$ (3 $\mu_{\rm B}$), while that of the V moment $\langle M_{\rm V} \rangle = 0.71(3)\mu_{\rm B}$, is much less than the expected value for $V^{3+}$ (2 $\mu_{\rm B}$) when it is fully polarized. The reduction of the V moment is due to strong frustration in the pyrochlore lattice of V ions, which is common in vanadium spinels. [2, 7, 16].

Four-circle neutron diffraction measurements on a $Co_{1.3}V_{1.7}O_4$ single crystal (#2) using a neutron wavelength of $\lambda = 2.4$ Å were also performed as a function of $T$ at several different Bragg $\mathbf{Q}$ points. As shown in Fig. 4 (a) and (b), upon cooling, the intensity of most of the Bragg peaks such as (400), (202), (313), (511) and (111) increase below 169 K $\sim T_{\rm C}$, exhibit a broad maximum at $\sim$ 100 K, and a dip at $\sim$ 40 K which is $T^*$ for $x = 0.3$. The (002) peak is a forbidden nuclear peak by the $Fd\bar{3}m$ symmetry and thus expected to be purely magnetic for stoichiometric $CoV_2O_4$. The (002) peak exhibits a gradual increase below $T_{\rm C}$ down to 10 K with a very weak dip at $\sim T^*$.

In order to understand the $T$-dependences of the nuclear and magnetic contributions at the Bragg reflections, we have performed two different measurements. Firstly, unpolarized four-circle diffraction using a neutron wavelength of $\lambda = 0.9$ Å was performed to reach high $\mathbf{Q}$ values where magnetic contributions are negligible due to the fall-off of the magnetic form factors of the $Co^{2+}$ and $V^{3+}$ ions. As shown in Fig. 4 (c), the high $Q$ Bragg peaks studied also exhibit similar $T$-dependences, and the dip at $T^* \sim 40$ K is more pronounced than the low $Q$ Bragg peaks shown in Fig. 4 (a) and (b). Thus, the observed dip of the Bragg peak intensities at $T^*$ is mainly due to a change in the signal of the nuclear Bragg peak, and possibly caused by the extinction effect on the diffraction intensities [29], which should be the largest at $T^*$ at which the distortion is minimal.

Secondly, we performed three-axis polarized neutron scattering measurements on the #2 $x = 0.3$ single crystal for the (002) Bragg peak. The crystal was aligned in the $(HHL)$ scattering plane and a vertical guide field of 3 T was applied along the [1,-1,0] direction. Upon cooling, the (002) non-spin-flip (NSF) and spin-flip (SF) scattering, $I_{\rm NSF}$ and $I_{\rm SF}$ respectively, gradually develops with decreasing $T$ below $T_{\rm C}$. Upon further cooling, it keeps increasing before the SF scattering starts decreasing at $T^* \sim 40$ K. As explained in details in the Supplementary Material[29], for offstroichiometric $x \neq 0$, the V-

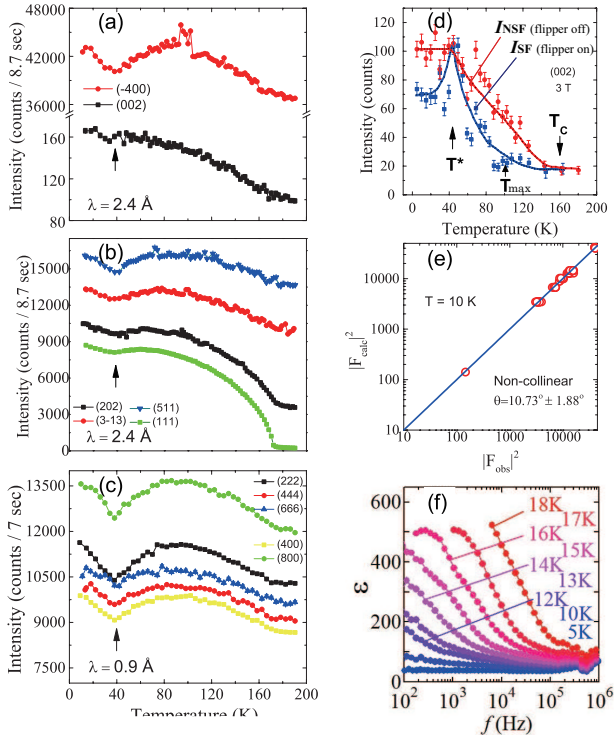


FIG. 4: (Color online) (a)(b) $T$ dependence of the measured intensity of Bragg peaks of $Co_{1.3}V_{1.7}O_4$ single crystal (#2) measured using neutron wavelength $\lambda = 2.4$ ÅThese Bragg peaks can be both nuclear and magnetic in origin due to the ferrimagnetic order. (c) The $T$ dependence of the Bragg peaks with large absolute value of momentum transfer $Q$, measured using $\lambda$ =0.9 Å, that are mainly nuclear. (d) $T$ dependence of the non-spin-flip ($I_{NSF}$) and the spin-flip ($I_{SF}$) intensity of (002) magnetic Bragg peak measured using polarized neutron with a vertical guide field of 3 T. The lines are a guide to the eye. (e) Single Crystal refinement of $Co_{1.3}V_{1.7}O_4$ (#2) at 10 K: Measured ($y$ axis) and calculated ($x$ axis) values for the absolute nuclear and magnetic structure factors of the Bragg peaks. (f) Frequency dependence of the dielectric constant for $Co_{1.21}V_{1.79}O_4$.

site is partially occupied by Co ions. Thus, in principle, both the coherent nuclear scattering due to the difference in the coherent nuclear scattering length of Co and V, and the magnetic scattering from the antiferromagnetic spin components along [1-10] and from the ferromagnetic component along the [001] direction (due to the different magnetic moments of Co and V ions) can contribute to $I_{NSF}(002)$. Since in the unpolarized neutron scattering measurement (Fig. 4), the nuclear reflections at high $Q$s also increase below $T_C$, the development of $I_{NSF}(002)$ below $T_C \sim 160$ K must be mainly nuclear due to the off-stoichiometry. On the other hand, $I_{SF}$ (002) is purely magnetic, which can contain the contribution from the FM components at the V-site due to the presence of the Co moments at the V-site as well as that from the AFM (canted) components at the V-site. Thus, the development of $I_{SF}$ below 100 K $\sim T_{max}$ can be understood as due to a canting of the moments at the V-site. In this scenario, the downturn of $I_{SF}$ below $T^* \sim 40$ K is due to the extinction effect. Another scenario is also possible, in which upon cooling $I_{SF}$ develops very weakly below $T_C$ due to the FM components of the Co and V moments at the V-site, and decreases below $T^*$ due to a canting of the moments at the V-site. The second scenario, however, is unlikely because similar decreases below $T^*$ were observed at the nuclear reflections at high $Q$s where magnetic scattering is negligible (see Fig. 4 (c)). Thus, we conclude that the canting of the V moments occurs well below $T_C$, most likely below $T_{max}$. By refining the 10 K single crystal unpolarized neutron diffraction data (see Fig. 4 (e)), the canting angle is determined to be $\sim 11(2)^\circ$, which is close to the value of $20(2)^\circ$ obtained from the powder diffraction. Such cantings of the $V^{3+}$ moments have been observed in the orbital solid states of the insulating $MnV_2O_4$ [6, 7] and $FeV_2O_4$ [16], and can be understood as an orbital ordering causes the anisotropic spin Hamiltonian between the $V^{3+}$ moments.

Unlike in the insulating compounds where the orbital solid order occurs in a first order fashion, the structural distortion in the spinel cobalt vanadate is subtle and gradual as a function of $T$, resulting in the glassy nature of the orbital order in the system. To confirm the slow dynamics associated with an orbital glass state, we have measured the dielectric constant as a function of frequency for $Co_{1.21}V_{1.79}O_4$ at various low $T$s. As shown in Fig. 4 (f), the data exhibits a frequency dependence similar to the behaviors observed in the orbital glass state of $FeCr_2S_4$ [31]. These data lead us to believe that a similar orbital glassy state must be realized in the nearly metallic spinel cobalt vanadate.

In summary, our systematic study of nearly metallic spinel cobalt vanadate $Co_{1+x}V_{2-x}O_4$ with various values of $x$ clarified that there are three characteristic temperatures in this compound, $T_C$ at which a ferrimagnetic ordering sets in, $T_{max}$ at which the elongation of the crystal is maximized, and $T^*$ below which the lattice distortion changes from elongation to contraction. The neutron scattering of $Co_{1.3}V_{1.7}O_4$ indicates that the canting of the V moments occurs below $\sim T_{max}$. The interesting gradual $T$-dependence of the subtle lattice distortion ($\Delta L/L \sim 10^{-4}$) correlated with the spin canting and the slow dynamics observed in $\epsilon$ indicate the existence of an orbital glassy state at low $T$s in this compound.

The work at Waseda University was partly supported by JSPS KAKENHI Grant No. 25287090. Research at UVA was supported by the US Department of Energy, Office of Basic Energy Sciences,Division of Materials Sciences and Engineering, under Award No. DE-FG02-07ER46384. We acknowledge the support of the National Institute of Standards and Technology, U. S. Department of Commerce, in providing the neutron research facilities for powder diffraction measurements used in this work. This research at ORNL's High Flux Isotope Reactor was

sponsored by the Scientific User Facilities Division, Office of Basic Energy Sciences, US Department of Energy.

* Email: sachithd83@gmail.com
† Email: katsuf@waseda.jp

[1] Y. Ueda, N. Fujiwara, and H. Yasuoka, J. Phys. Soc. Jpn. **66**, 778 (1997).
[2] S.-H. Lee, D. Louca, H. Ueda, S. Park, T. J. Sato, M. Isobe, Y. Ueda, S. Rosenkranz, P. Zschack, J. I. niguez, et al., Phys. Rev. Lett. **93**, 156407 (2004).
[3] Z. Zhang, D. Louca, A. Visinoiu, S.-H. Lee, J. D. Thompson, T. Proffen, A. Llobet, Y. Qiu, S. Park, and Y. Ueda, Phys. Rev. B **74**, 014108 (2006).
[4] T. Suzuki, M. Katsumura, K. Taniguchi, T. Arima, and T. Katsufuji, Phys. Rev. Lett. **98**, 127203 (2007).
[5] H. D. Zhou, J. Lu, and C. R. Wiebe, Phys. Rev. B **76**, 174403 (2007).
[6] J. H. Chung, J. H. Kim, S. H. Lee, T. J. Sato, T. Suzuki, M. Katsumura, and T. Katsufuji, Phys. Rev. B **77**, 054412 (2008).
[7] V. O. Garlea, R. Jin, D. Mandrus, B. Roessli, Q. Huang, M. Miller, A. J. Schultz, and S. E. Nagler, Phys. Rev. Lett. **100**, 066404 (2008).
[8] V. Hardy, Y. Bréard, and C. Martin, Phys. Rev. B **78**, 024406 (2008).
[9] S.-H. Baek, N. J. Curro, K.-Y. Choi, A. P. Reyes, P. L. Kuhns, H. D. Zhou, and C. R. Wiebe, Phys. Rev. B **80**, 140406 (2009).
[10] S. Sarkar, T. Maitra, R. Valentí, and T. Saha-Dasgupta, Phys. Rev. Lett. **102**, 216405 (2009).
[11] G.-W. Chern, N. Perkins, and Z. Hao, Phys. Rev. B **81**, 125127 (2010).
[12] Y. Nii, N. Abe, and T. Arima, Phys. Rev. B **87**, 085111 (2013).
[13] S. L. Gleason, T. Byrum, Y. Gim, A. Thaler, P. Abbamonte, G. J. MacDougall, L. W. Martin, H. D. Zhou, and S. L. Cooper, Phys. Rev. B **89**, 134402 (2014).
[14] T. Katsufuji, T. Suzuki, H. Takei, M. Shingu, K. Kato, K. Osaka, M. Takata, H. Sagayama, and T. Arima, J. Phys. Soc. Jpn. **77**, 053708 (2008).
[15] S. Sarkar and T. Saha-Dasgupta, Phys. Rev. B **84**, 235112 (2011).
[16] G. J. MacDougall, V. O. Garlea, A. A. Aczel, H. D. Zhou, and S. E. Nagler, Phys. Rev. B **86**, 060414 (2012).
[17] Q. Zhang, K. Singh, F. Guillou, C. Simon, Y. Breard, V. Caignaert, and V. Hardy, Phys. Rev. B **85**, 054405 (2012).
[18] Y. Nii, H. Sagayama, T. Arima, S. Aoyagi, R. Sakai, S. Maki, E. Nishibori, H. Sawa, K. Sugimoto, H. Ohsumi, et al., Phys. Rev. B **86**, 125142 (2012).
[19] J.-S. Kang, J. Hwang, D. H. Kim, E. Lee, W. C. Kim, C. S. Kim, S. Kwon, S. Lee, J.-Y. Kim, T. Ueno, et al., Phys. Rev. B **85**, 165136 (2012).
[20] S. Kawaguchi, H. Ishibashi, S. Nishihara, M. Miyagawa, K. Inoue, S. Mori, and Y. Kubota, J. Phys.: Condens. Matter **25**, 416005 (2013).
[21] Z. H. Huang, X. Luo, L. Hu, S. G. Tan, Y. Liu, B. Yuan, J. Chen, W. H. Song, and Y. P. Sun, J. Appl. Phys. **115**, 034903 (2014).
[22] D. Choudhury, T. Suzuki, D. Okuyama, D. Morikawa, K. Kato, M. Takata, K. Kobayashi, R. Kumai, H. Nakao, Y. Murakami, et al., Phys. Rev. B **89**, 104427 (2014).
[23] A. Kismarahardja, J. S. Brooks, A. Kiswandhi, K. Matsubayashi, R. Yamanaka, Y. Uwatoko, J. Whalen, T. Siegrist, and H. D. Zhou, Phys. Rev. Lett. **106**, 056602 (2011).
[24] A. Kiswandhi, J. S. Brooks, J. Lu, J. Whalen, T. Siegrist, and H. D. Zhou, Phys. Rev. B **84**, 205138 (2011).
[25] Y. Huang, Z. Yang, and Y. Zhang, J. Phys., Condens. Matter **24**, 056003 (2012).
[26] R. Kaur, T. Maitra, and T. Nautiyal, J. Phys.: Condens. Matter **26**, 045505 (2014).
[27] A. Kismarahardja, J. S. Brooks, H. D. Zhou, E. S. Choi, K. Matsubayashi, , and Y. Uwatoko, Phys. Rev. B **87**, 054432 (2013).
[28] J. Ma, J. H. Lee, S. E. Hahn, T. Hong, H. B. Cao, A. A. Aczel, Z. L. Dun, M. B. Stone, W. Tian, Y. Qiu, et al., Phys. Rev. B **91**, 020407 (2015).
[29] See the Supplementary material.
[30] D. R. i Plessis, D. Casavant, V. O. Garlea, A. A. Aczel, M. Feygenson, J. Neuefeind, H. D. Zhou, S. E. Nagler, , and G. J. MacDougall, cond-mat. p. 1507.02572 (2015).
[31] R. Fichtl, V. Tsurkan, P. Lunkenheimer, J. Hemberger, V. Fritsch, H.-A. K. von Nidda, E.-W. Scheidt, and A. Loidl, Phys. Rev. Lett. **94**, 027601 (2005).